

## Self-consistent numerical study of pure and impurity doped three-band Hubbard model

PRASENJIT SEN and AVINASH SINGH

Department of Physics, Indian Institute of Technology, Kanpur 208 016, India

Email: prasen@iitk.ernet.in

MS received 24 December 1996

**Abstract.** The three-band Hubbard model – both pure and with static non-magnetic impurities – has been studied within a self-consistent numerical Hartree–Fock (HF) scheme. The system shows nesting properties only in the absence of direct O–O hopping. Spin excitations in the system are gapless with the existence of a Goldstone mode in the broken-symmetry state. The variation of spin-wave velocity with Cu-site Coulomb repulsion shows a  $(1/(2U_d) + 1/\Delta)$  dependence in the strong-coupling limit. Each non-magnetic impurity in the system gives rise to two gap states for a particular spin and the local moment produced is robust even at finite concentration of mobile hole doping. The gapless Goldstone mode is preserved even in case of unequal concentration of impurities on the two sublattices.

**Keywords.** Three-band Hubbard model; charge-transfer insulator; Mott–Hubbard insulator; high  $T_c$  superconductor; impurity.

**PACS Nos** 71.27; 71.55; 75.10; 75.20

### 1. Introduction

The three-band Hubbard model has been proposed by many authors [1, 2] as a minimal model for describing the physical properties of the copper-oxide planes in high-temperature superconductors. Extensive studies that have been done on this model were motivated by the observation that the undoped parent compounds of the superconducting cuprates are charge-transfer insulators (CTI) rather than Mott–Hubbard (MH) insulators.

It has been argued that this model can be reduced to an effective one-band Hubbard model in order to describe the low-energy physics of the copper-oxide planes when only the spin degrees of freedom are important. A number of studies of the magnetic properties of the copper-oxide planes have been done within a one-band Hubbard model. But recently, lot of experiments have been done on the high- $T_c$  cuprates doped with static, and in particular non-magnetic impurities like  $Zn^{2+}$ ,  $Al^{3+}$ ,  $Ga^{3+}$  etc., and although some of the properties of these systems have been understood within a one-band model, others require a more detailed picture like the three-band model for their understanding.

It has been established through susceptibility [3] measurements that non-magnetic impurities substituting Cu in the copper-oxide planes generate local moments. NMR [4, 5] measurements show that moments form on the neighbouring Cu sites. Other effects that these impurities have include a rapid reduction in superconducting transition

temperature ( $T_c$ ) [4], onset of insulating behavior in the metallic state [6], a reduction in Néel temperature  $T_N$  [7] and spin-glass behavior in the insulating state [7]. Microscopic understanding of some of these effects have been gained by studying the effects of static non-magnetic impurities in MH insulators described by one-band Hubbard model. Within a HF description of the Hubbard model, the impurity-problem has been studied both analytically within a  $T$ -matrix analysis in the limit of large impurity potential [9] and within a self-consistent numerical procedure on finite-sized systems [10]. In both cases gap-states localized around the impurity sites are produced for a particular spin, depending on the sublattice of impurity substitution. These states, when occupied with electrons, give rise to local moments.

In one-band Hubbard model in hole picture the gap state is formed slightly below the upper Hubbard band (UHB), between the two bands. This being the lowest unoccupied state for the Cu  $3d$  holes, the first added hole goes into this state and the moment is lost. At temperatures comparable to the energy difference between the gap state and the lower edge of the UHB, part of the moment can be recovered due to thermal excitation of the hole from the gap state to the UHB [11]. But how the moment survives at low temperatures and finite concentration of mobile hole doping is not clear.

In this paper we consider the full three-band Hubbard model description of the Cu  $3d$  holes in the copper-oxide planes in the insulating state when there is exactly one electron (or equivalently one hole) per copper site and present a self-consistent numerical study of the antiferromagnetic (AF) state. In the absence of direct O–O hopping the pure system shows an antiferromagnetic ordering as soon as there is a non-zero Coulomb repulsion on the Cu sites ( $U_d$ ). For non-zero O–O hopping a critical value of  $U_d$  is required for the AF order to set in. With the generally accepted set of values for the parameters, the system is CTI at the half-filled level. It has three bands—lower and upper Hubbard bands at the bottom and the top and the oxygen band in the middle. Each non-magnetic impurity in the three-band model gives rise to two gap-states—one slightly below the UHB and one below the oxygen band. Oxygen band being lower in energy, the upper gap-state remains occupied even at finite hole dopings making the moment robust.

We have also studied the nature of spin-wave excitation in the system. In the pure case the spin-wave excitation is gapless and one has a Goldstone mode. For  $U_d \gg t_{pd}$  the spin-wave velocity increases with decreasing  $U_d$  showing roughly a  $((1/2U_d) + (1/\Delta))$  dependence as in the equivalent Heisenberg model. The Goldstone mode is preserved even in presence of impurities.

## 2. Pure system

We consider the following three-band Hubbard Hamiltonian for the  $3d$  holes in the copper-oxide planes, which is shown in figure 1 (adapted from ref. [14])

$$\begin{aligned}
 H = & -t_{pd}^{ij} \sum_{\langle i,j \rangle; \sigma} (p_{i\sigma}^\dagger d_{j\sigma} + \text{h.c.}) - t_{pp}^{ij} \sum_{\langle l,m \rangle; \sigma} (p_{l\sigma}^\dagger p_{m\sigma} + \text{h.c.}) + \epsilon_p \sum_{i\sigma} p_{i\sigma}^\dagger p_{i\sigma} \\
 & + \epsilon_d \sum_{i\sigma} d_{i\sigma}^\dagger d_{i\sigma} + U_d \sum_i n_{i\uparrow}^d n_{i\downarrow}^d + U_p \sum_i n_{i\uparrow}^p n_{i\downarrow}^p + U_{pd} \sum_{\langle i,j \rangle} n_i^p n_j^d, \quad (1)
 \end{aligned}$$

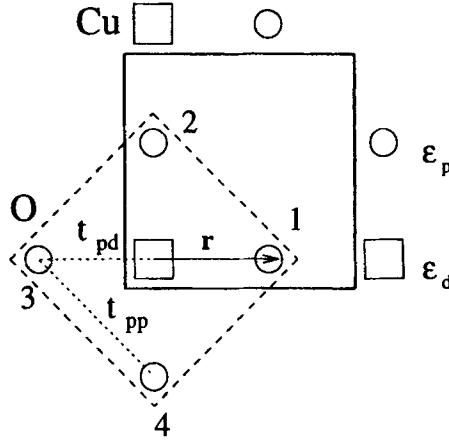


**Figure 1.** Basis (solid line bounded square) and  $\text{CuO}_4$  plaquette (dashed line bounded square) of the  $\text{CuO}_2$  plane of the three-band Hubbard model. The squares and the circles mark the Cu  $3d_{x^2-y^2}$  and O positions, at energies  $\epsilon_d$  and  $\epsilon_p$ , respectively. The  $2p_x$  and  $2p_y$  orbitals are located at 1,3 and 2,4,  $t_{pd}^{ij}$  denotes the transfer integral between copper and oxygen and  $t_{pp}^{ij}$  the direct oxygen hopping. The lattice spacing  $a = 2|r|$ .

where  $p(p^\dagger)$  and  $d(d^\dagger)$  are the annihilation (creation) operators for holes on the O and Cu sites,  $\langle i, j \rangle$  are nearest neighbour (nn) Cu and O sites and  $\langle l, m \rangle$  are two neighboring O sites;  $n$ 's are the respective number densities.  $t_{pd}$  is the hopping term between neighboring Cu  $3d$  and O  $2p$  orbitals and  $t_{pp}$  is the hopping matrix element between two nn O  $2p$  orbitals.  $\epsilon_d$  and  $\epsilon_p$  are the on-site energies of a hole sitting on Cu  $3d$  or O  $2p$  orbital.  $U_d$  and  $U_p$  are the Coulomb repulsion terms on the Cu and O sites respectively.  $U_{pd}$  is the repulsion between charges on the neighbouring Cu and O sites.  $\sigma$  is the spin index. The so called charge-transfer gap  $\Delta$  denotes the energy difference between oxygen and copper,  $\Delta \equiv \epsilon_p - \epsilon_d$ . In the hole picture  $\Delta$  is positive. The orbital symmetries of the type  $d_{x^2-y^2}$  and  $p_{x,y}$  imply additional phase factors for the hopping integrals  $t_{pd}^{ij}$  and  $t_{pp}^{ij}$ ,

$$\begin{aligned} t_{pd}^{0j} &= \phi^j t_{pd}, & \phi^1 &= \phi^2 = -1, & \phi^3 &= \phi^4 = 1, \\ t_{pp}^{ij} &= \psi^{ij} t_{pp}, & \psi^{12} &= \psi^{34} = -1, & \psi^{23} &= \psi^{41} = 1, \end{aligned}$$

where 0 labels the central copper and 1, 2, 3, 4 the four oxygen sites on the plaquette. In this section we shall be talking about a half-filled system when we have exactly one hole per copper site.

For all our calculations we take  $t_{pd} = 1.3 \text{ eV}$ ,  $\Delta = 3.0 \text{ eV}$ ,  $U_p = 0 \text{ eV}$  and  $U_{pd} = 0 \text{ eV}$  and a  $10 \times 10$   $\text{CuO}_2$  lattice. A more detailed discussion on the choice of the values of parameters is given in the section on doped system. In the HF approximation relevant to symmetry breaking along  $z$ -direction only, the interaction terms can be written as  $U \langle n_{i\uparrow} \rangle n_{i\downarrow} + U \langle n_{i\downarrow} \rangle n_{i\uparrow}$ , so that the on-site energy of spin  $\bar{\sigma} \equiv -\sigma$  hole on the  $i$ th Cu site is  $U \langle n_{i\bar{\sigma}} \rangle$ . In the site basis, matrix elements of the Hamiltonian for spin  $\sigma$  are given by  $\langle i | H_\sigma | i \rangle = \epsilon_d + U_d \langle n_{i\bar{\sigma}} \rangle$  if  $i$  is a Cu site and  $\langle i | H_\sigma | i \rangle = \epsilon_p + U_p \langle n_{i\bar{\sigma}} \rangle$  if  $i$  is an oxygen site.  $\langle i | H_\sigma | j \rangle = \pm t_{pd}$  if  $i$  and  $j$  are nn Cu and O sites and  $\langle l | H_\sigma | m \rangle = \pm t_{pp}$  if  $l$  and  $m$

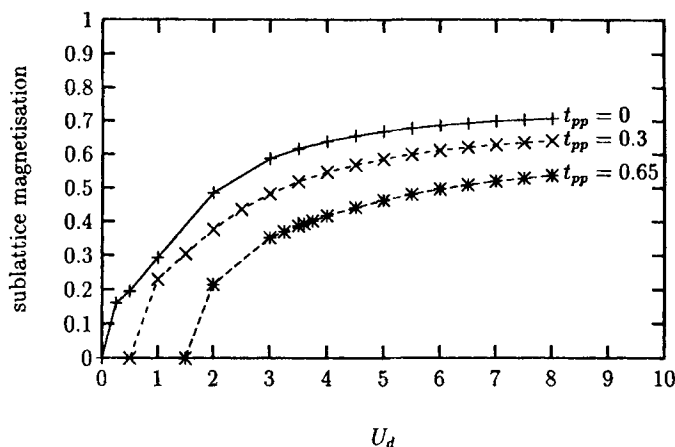


**Figure 2.** Sublattice magnetization as a function of  $U_d$  for different values of  $t_{pp}$  (all energies in eV).

are two nn O sites. Choice of an initial configuration of spin  $\bar{\sigma}$  densities on the Cu sites gives the starting Hamiltonian matrix  $H_\sigma$  which is diagonalized to give the eigensolutions  $E_{l\sigma}$ ,  $\phi_{l\sigma}$ . From these the spin densities are evaluated using  $\langle n_{i\sigma} \rangle = \sum_{E_{l\sigma} < E_F} (\phi_{l\sigma}^i)^2$ .  $H_\sigma$  is updated from these computed spin densities and the procedure is continued till self-consistency is achieved.

Exact numerical (QMC) calculations reveal that the three-band Hubbard model with a finite positive  $U_d$  possesses an AF ground-state [8]. In order to study the magnetic behavior of the system with changing  $U_d$  we have calculated the sublattice magnetization as a function of  $U_d$ . Figure 2 shows the variation of sublattice magnetization as a function of  $U_d$  for different values of  $t_{pp}$ . For  $t_{pp} = 0$  the system goes into an AF state for any finite positive  $U_d$ . This is because of nesting of the Fermi surface. When  $t_{pp} \neq 0$  the system loses its nesting property and a critical value of  $U_d$  is required for the system to become antiferromagnetic. This critical value of  $U_d$  increases with  $t_{pp}$ .

A study of the energy spectrum of the system shows that for large values of  $U_d$  ( $U_d \gg \Delta$ ) the system is a CTI. For an  $L \times L$   $\text{CuO}_2$  lattice, having  $L^2$  Cu and  $2L^2$  O sites, the first  $L^2/2$  states form the lower Hubbard band (LHB). The oxygen  $2p$  band in the middle has  $2L^2$  states and the UHB has another  $L^2/2$  states. The  $2p$  band is further split into three sub-bands similar to Zhang–Rice singlet-triplet splitting. The singlet sub-band lies below the bare oxygen energy, there are a group of non-bonding (NB) states at the bare oxygen energy  $\epsilon_p$  and the triplet sub-band lies above these NB states. For  $U_d < \Delta$  but above the critical value so that the system is an AF, the UHB goes below the oxygen band. The charge-gap is maintained and the system is a MH insulator. Below the critical value of  $U_d$  when the sublattice magnetization vanishes, the charge-gap also disappears and the system becomes a  $d$ -type metal. There are no singlet-triplet splitting in the oxygen band in these cases (figure 3). The situation in intermediate range of values of  $U_d$  is more complicated because the UHB and the oxygen band are strongly mixed.

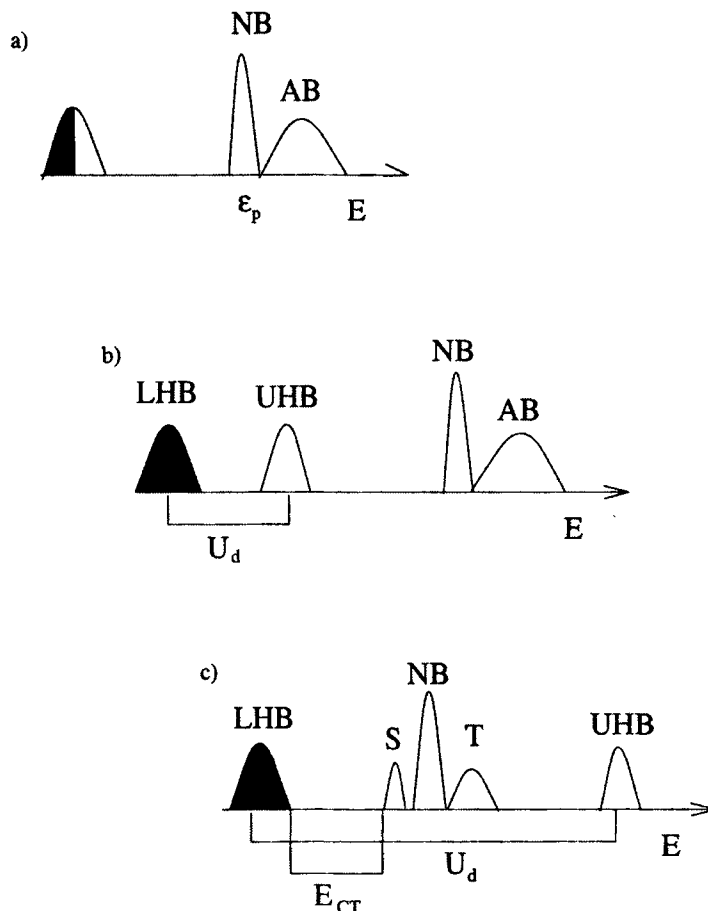


**Figure 3.** Single-particle spectra for the three-band Hubbard model in the hole picture: (a) metal, (b) Mott-Hubbard insulator, (c) charge-transfer insulator with a singlet-triplet splitting. Shaded regions denote the occupied states.  $[N](A)B = [\text{non}](\text{anti})\text{bonding}$ ,  $S = \text{singlet}$ ,  $T = \text{triplet}$ ,  $E_{CT}$  = renormalised charge-transfer gap.

Spin waves are the low-energy collective excitations representing the transverse spin fluctuation in the AF ground state. In the one-band Hubbard model and its strong-coupling analogue, the Heisenberg model, the nature of spin excitations has been studied extensively. It is well known that in these systems the spin-wave spectrum is gapless with the existence of a Goldstone mode. The dispersion for the long-wavelength spin-wave modes is linear in the momentum  $Q$ . The spin-wave modes are obtained from the poles of the time-ordered transverse spin propagator  $\langle T[S^-(i, t)S^+(j, t')] \rangle$  which, in the random phase approximation (RPA), has the form  $[\chi^{-+}(\Omega)] = [\chi_0^{-+}(\Omega)] / (1 - U[\chi_0^{-+}(\Omega)])$ . The matrix elements of  $[\chi_0^{-+}(\Omega)]$ , the bare antiparallel-spin particle-hole propagator, are given by

$$[\chi_0^{-+}(\Omega)]_{ij} = i \int_{-\infty}^{\infty} \frac{d\omega}{2\pi} g_{ij}^{\uparrow}(\omega) g_{ji}^{\downarrow}(\omega - \Omega), \quad (2)$$

where  $g$ 's are the Green's functions in the AF state. In terms of the eigensolutions  $E_l, \phi_l$  in the self-consistent state  $\chi_0^{-+}(\Omega)$  has the form

$$[\chi_0^{-+}(\Omega)]_{ij} = \sum_{\substack{E_l < E_F \\ E_l > E_F}} \frac{\phi_{l\uparrow}^i \phi_{l\uparrow}^j \phi_{m\downarrow}^i \phi_{m\downarrow}^j}{E_{l\uparrow} - E_{m\downarrow} - \Omega} + \sum_{\substack{E_l > E_F \\ E_l < E_F}} \frac{\phi_{l\uparrow}^i \phi_{l\uparrow}^j \phi_{m\downarrow}^i \phi_{m\downarrow}^j}{E_{m\downarrow} - E_{l\uparrow} + \Omega}. \quad (3)$$

Since only the Cu spins form AF order, spin-waves will have amplitude only on the Cu sites, and so we calculate  $[\chi_0^{-+}(\Omega)]_{ij}$  connecting only the Cu sites. In (3) the site indices  $i$  and  $j$  thus run only through the Cu sites, but the eigenvalue indices  $l$  and  $m$  run through all three bands.

All information regarding the nature of the spin-wave excitations is contained in the eigensolutions of  $[\chi_0^{-+}(\Omega)]$ , as is evident from the expansion of the full RPA susceptibility given below in terms of the eigenvalues  $\lambda(\Omega)$  and the eigenvectors  $|\phi_\lambda(\Omega)\rangle$  of  $[\chi_0^{-+}(\Omega)]$ . The spin-wave energies are obtained from the pole  $1 - U\lambda(\Omega) = 0$  in the RPA spin susceptibility, and the eigenvector yields the spin-wave amplitude

$$[\chi^{-+}(\Omega)] = \sum_{\lambda} \frac{\lambda |\phi_\lambda(\Omega)\rangle \langle \phi_\lambda(\Omega)|}{1 - U\lambda(\Omega)}. \quad (4)$$

In the three-band model, as in the one-band model, the largest eigenvalue  $\lambda_{\max}(\Omega = 0)$  of the  $[\chi_0^{-+}(\Omega)]$  matrix for  $\Omega = 0$  is found to be exactly equal to  $1/U_d$ , confirming that the spin-wave excitations are gapless.

The higher ( $n$ th) spin-wave mode energies  $\Omega_n$  are determined by solving  $1 - U\lambda_n(\Omega_n) = 0$  for the appropriate ( $n$ th from the top) eigenvalue  $\lambda_n(\Omega)$ . The root of the equation  $1 - U\lambda_n(\Omega_n) = 0$  is determined by obtaining  $\lambda_n(\Omega)$  for several close values of  $\Omega$  on both sides of the root and then linearly interpolating between them. Thus if  $(\lambda_n^1, \Omega_n^1)$  and  $(\lambda_n^2, \Omega_n^2)$  are two sets of values of two  $\Omega$ 's very close to and on either side of the root, then the root  $\Omega_n$  is determined from

$$\lambda(\Omega_n) = \frac{1}{U} = \lambda_n^1 + \frac{\lambda_n^2 - \lambda_n^1}{\Omega_n^2 - \Omega_n^1} (\Omega_n - \Omega_n^1). \quad (5)$$

The procedure involves first obtaining the self-consistent state for the system and then the process of constructing and diagonalizing the  $[\chi_0^{-+}(\Omega)]$  matrix for different values of  $\Omega$ . From the set of eigenvalues  $\lambda_n(\Omega)$ , the spin-wave energies are then obtained as above. Nature of spin-wave modes can be studied by obtaining the angles of rotation of local spin vectors from the spin-wave amplitudes and the local magnetization  $S_z^i$  using [12]

$$\theta_i = \sin^{-1} \frac{\phi_\lambda^i}{S_z^i}. \quad (6)$$

The  $\Omega_0 = 0$  mode corresponds to a spin-wave excitation which has equal amplitudes on all sites and rotates all the spins by equal angles and is identified as the Goldstone mode. Thus, as in the one-band model, the spin-wave excitation in a three-band model is gapless and there exists a Goldstone mode as one would expect in a system with continuous spin-rotational symmetry.

Spin-wave modes can be assigned mode numbers [10] which yield wave vectors  $Q_{x/y} = (2\pi/L)n_{x/y}$ . The spin-wave energy is found to be proportional to the wave vector

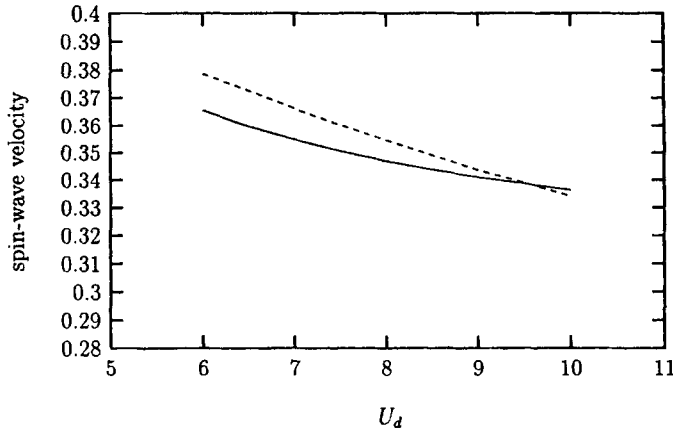


**Figure 4.** Spin-wave velocity (in eV) obtained at the RPA level for the finite-size system (dashed line) and calculated from analytical results of literature (continuous line) as a function of  $U_d$  (in eV).

for the long-wavelength modes (modes for a few  $\lambda$ 's at the top) in the strong-coupling ( $U_d \gg t_{pd}$ ) limit. The spin-wave velocity  $v$  can be defined by  $\Omega_Q = vQ$  in the long-wavelength limit, where  $Q = (2\pi/L)\sqrt{n_x^2 + n_y^2}$  is the magnitude of the wave vector. The spin-wave energy scale in the problem is set by the exchange coupling  $J$  between nn Cu atoms in the equivalent Heisenberg model to which the three-band Hubbard model can be mapped in the limit  $U_d \gg t_{pd}$  and  $\Delta \gg t_{pd}$ . The spin-wave velocity is then equal to  $\sqrt{2}Ja$ , where  $a$  is the lattice constant, set equal to unity henceforth. The effective exchange coupling for a three-band Hubbard model is given by [13]

$$J = \left( \frac{2t_{pd}^4}{\Delta^2} \right) \left( \frac{1}{2U_d} + \frac{1}{\Delta} \right). \quad (7)$$

In figure 4 we plot the spin-wave velocity, calculated from the energy of the first spin-wave mode, for which  $n_x = 1, n_y = 0$  (or equivalently  $n_x = 0, n_y = 1$ ), and also  $\sqrt{2}J$  calculated from eq. (7). For large values of  $U_d$  the spin-wave velocity calculated from our model is found to be in reasonable agreement with the analytical result. The slight disagreement is not surprising as the condition  $\Delta \gg t_{pd}$  is not really satisfied in this case. On a finite lattice the  $Q$ -space is discrete and the first mode corresponds to a  $Q$  of 0.62 for a  $10 \times 10$  system. Below  $U_d$  of 6.0, spin-wave energy no longer remains linear for this  $Q$  and calculation of spin-wave velocity from the simple relation  $\Omega_Q = vQ$  is not possible.

### 3. Impurity-doped system

We have studied the problem of static non-magnetic impurities doped in the three-band Hubbard model. As in the one-band case we model the impurities by putting a high repulsive potential on the impurity (Cu) site [9] to restrict the Cu 3d holes from

occupying that site. The Hamiltonian now is

$$H = H_{\text{pure}} + V \sum_{I,\sigma} a_{I\sigma}^\dagger a_{I\sigma}, \quad (8)$$

where  $H_{\text{pure}}$  is the Hamiltonian for the pure system given by (1) and  $I$  runs over the impurity sites.

The values of most of the parameters of the model are related to electron spectroscopy and are obtained from comparison with the results of these experiments. Different kinds of theoretical techniques give slightly different sets of values. But a generally acceptable set of values is [14]  $t_{pd} = 1.3$  eV,  $t_{pp} = 0.65$  eV,  $U_d = 8.8$  eV,  $U_p = 0$  eV,  $U_{pd} = 0$  eV,  $\Delta = 3.0$  eV. In this section we work with this set of values of the parameters.

Starting from the pure system at half-filling one Cu  $3d$  hole is removed for each added impurity. For each impurity, depending on the sublattice of its substitution, a self-consistent solution of this Hamiltonian shows that in the spectrum of one particular spin there are three states outside the bands and for the other there is one outside. Consider an impurity on an  $A$ -sublattice site (having majority of  $\uparrow$ -spin holes), in an  $L \times L$  system. In the  $\uparrow$ -spin spectrum there are  $(L^2/2 - 1)$  states in the LHB. One state goes out to the defect state which is the highest in energy ( $\sim V$ ). The oxygen band and the UHB have  $(2L^2 - 1)$  and  $(L^2/2 - 1)$  states respectively, one state from each going out to form the gap states. The  $L^2/2$ th and the  $2L^2$ th states are the two gap states. In the spectrum for the  $\downarrow$ -spin hole, the LHB and the oxygen band remain unaffected. The UHB has  $(L^2/2 - 1)$  states, one state going to the defect state. The situation is simply reversed if the impurity is placed on a  $B$ -sublattice site. Coming to the nature of these states, we find that the defect state is essentially site-localized on the impurity site, whereas the lower gap state, coming out of the oxygen band, has amplitude mainly on the oxygen sites around the impurity, and the upper gap state has amplitude mainly on the four Cu sites neighbouring the impurity. In this respect the upper gap state is similar to the gap state in a one-band model [9, 10]. This state, when occupied by electrons, creates a local moment residing predominantly on the four Cu sites neighbouring the impurity. The defect state has amplitude primarily on the impurity site. With only a non-magnetic impurity on an  $A$ -sublattice and no extra added hole, the system has  $(L^2/2 - 1)$   $\uparrow$ -spin and  $L^2/2$   $\downarrow$ -spin holes. So the LHB is completely filled and all the other states are empty of holes. The lower gap state being the lowest unoccupied state for the holes, the first added  $\uparrow$ -spin hole goes into this state and subsequent holes go into the oxygen band. So even at finite concentration of mobile hole doping the upper gap state remains occupied by electrons. Thus unlike in one-band model, the local moment in three-band model is robust with respect to mobile hole doping. In figure 5 we show the variations of the two energy gaps—between lower gap-state and oxygen band and the upper gap-state and the UHB. It is interesting to note that although the lower gap varies considerably, the upper gap is relatively insensitive to the variation of  $V$ .

The magnitude of the local moment is proportional to the density of the gap state on the copper sites. We find that the total density of the upper gap state on the copper sites is less than 1. Part of the density goes out to the oxygen sites because of the Cu–O hybridization. This explains the observation that the measured moment is less than the theoretically expected value [3]. If one spin is removed from a compensated spin system like an AF, the resulting moment should be that due to a spin- $\frac{1}{2}$  electron, which is

*Self-consistent numerical study*

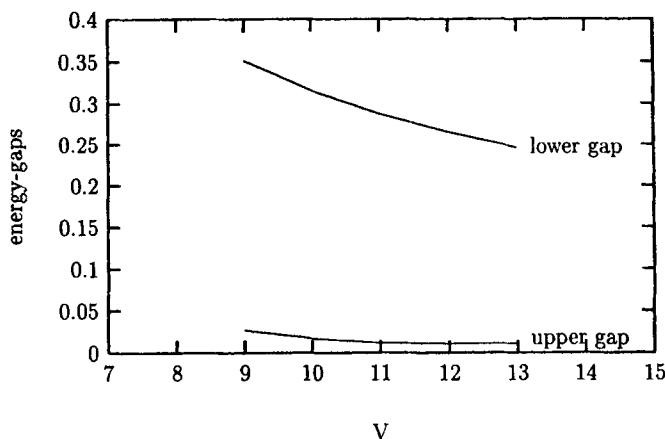


**Figure 5.** Variation of the two energy-gaps with  $V$  (all in eV).

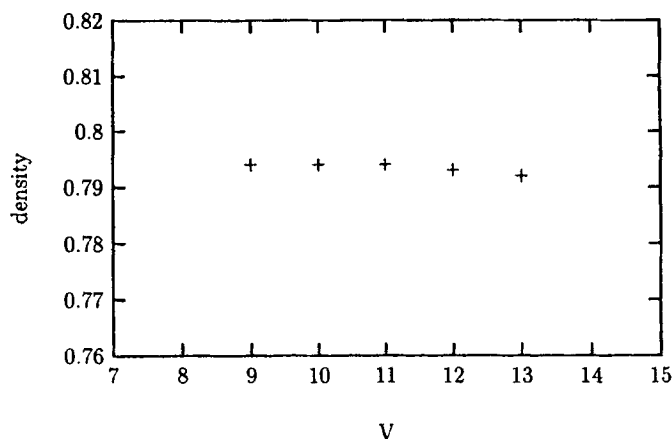


**Figure 6.** Gap-state density on the Cu-sites for different impurity potential  $V$  (in eV).

$(g\sqrt{s(s+1)}) = 1.9\mu_B$ . But in experiments the moment is measured to be  $1.2\mu_B$ , about 35% less than the calculated value. More importantly this is found to be independent of the nature of the non-magnetic impurity,  $Zn^{2+}$ ,  $Al^{3+}$ ,  $Ga^{3+}$ —all are seen to give rise to moment of about the *same* magnitude. In our calculations we find that about 21% of the gap-state density escapes to the oxygen sites from copper. Figure 6 shows total density of the second gap state on Cu sites which is interestingly found to be essentially constant over the range of  $V$  studied in our calculations. This leads to the significant conclusion that the gap-state-induced moment is more or less independent of the details of the non-magnetic impurity within our model of the impurity potential term.

We have also studied the nature of spin-wave excitations in the impurity-doped system. We find that the gapless Goldstone mode associated with spontaneous symmetry-breaking in the AF ground state is preserved in presence of impurities and even when the concentration of impurities on the two sublattices are not equal. This is because the  $SU(2)$

symmetry of the Hamiltonian, which is broken in the AF ground state, is still preserved. Wan *et al* [15] have obtained two modes of spin-wave excitation in case of unequal concentration of impurities on the two sublattices. We think the gapless mode in our calculation actually corresponds to their acoustic mode.

#### 4. Conclusion

We have studied the pure and impurity-doped three-band Hubbard models. When direct O–O hopping is not present the pure system shows nesting property and goes into an AF state for any non-zero  $U_d$ . In presence of a finite  $t_{pp}$  the nesting is lost and the system becomes an AF only above a certain critical value of  $U_d$ , which increases with  $t_{pp}$ . The transverse spin excitations in the system have a gapless Goldstone mode. The spin-wave velocity, in the strong-coupling limit, shows a  $((1/2U_d) + (1/\Delta))$  dependence in agreement with the strong-coupling perturbative approach.

In the doped system each non-magnetic impurity produces two gap states. The upper gap state remains occupied by electrons even in presence of finite concentration of mobile holes so that the local moment formed is robust. The density of the occupied gap state on the Cu sites is less than 1, so that the local moment is less than the theoretical value of  $1.9 \mu_B$ . The local moment is found to be insensitive to the impurity-potential  $V$  suggesting that the observed moment is independent of the detailed nature of the impurity. Even with unequal concentration of impurities on two sublattices, the spin-wave excitation remains gapless, and the Goldstone mode is also preserved.

#### References

- [1] V J Emery, *Phys. Rev. Lett.* **58**, 2794 (1987)
- [2] C M Varma, S Schmitt-Rink and E Abrahams. *Solid State Commun.* **62**, 681 (1987)
- [3] G Xiao, M Z Cieplak, J Q Xiao and C L Chien, *Phys. Rev.* **B42**, 8752 (1990)
- [4] R E Walstedt, R F Bell, L F Schneemeyer and J V Waszczak. *Phys. Rev.* **B48**, 10646 (1993)
- [5] A V Mahajan, H Alloul, G Collin and J F Marucco, *Phys. Rev. Lett.* **72**, 3100 (1994)
- [6] G Xiao, M Z Cieplak, A Gravin, F H Stritz, A Bakhshai and C L Chien, *Phys. Rev. Lett.* **60**, 1446 (1988)
- [7] B Keimer, A Aharony, A Auerbach, R J Birgeneau, A Cassanho, Y Endoh, R W Erwin, M A Kastner and G Shirane, *Phys. Rev.* **B45**, 7430 (1992)
- [8] G Dopf, A Maramatsu and W Hanke, *Europhys. Lett.* **17**, 559 (1992)
- [9] P Sen, S Basu and A Singh, *Phys. Rev.* **B50**, 10381 (1994)
- [10] S Basu and A Singh, *Phys. Rev.* **B53**, 6406 (1996)
- [11] P Sen and A Singh (unpublished)
- [12] A Singh and Z Tešanović, *Phys. Rev.* **B41**, 614 (1990)
- [13] J Zaanen and A Olés, *Phys. Rev.* **B37**, 9423 (1988)
- [14] W Brenig, *Phys. Rep.* **251**, 179 (1995)
- [15] C C Wan, A B Harris and D Kumar, *Phys. Rev.* **B48**, 1036 (1993)